

## Communication

# Design, Synthesis and 5-HT<sub>1A</sub> Binding Affinity of *N*-(3-(4-(2-Methoxyphenyl)piperazin-1-yl)propyl)tricyclo[3.3.1.1<sup>3,7</sup>]decan-1-amine and *N*-(3-(4-(2-Methoxyphenyl) piperazin-1-yl)propyl)-3,5-dimethyl-tricyclo[3.3.1.1<sup>3,7</sup>]decan-1-amine

Grigoris Zoidis <sup>1,\*</sup>, María Isabel Loza <sup>2</sup> and Marco Catto <sup>3</sup>

<sup>1</sup> Department of Pharmacy, Division of Pharmaceutical Chemistry, School of Health Sciences, National and Kapodistrian University of Athens, Panepistimiopolis Zografou, 15771 Athens, Greece

<sup>2</sup> BioFarma Research Group, Centro Singular de Investigación en Medicina Molecular y Enfermedades Crónicas (CIMUS), Universidade de Santiago de Compostela, 15782 Santiago de Compostela, Spain; mabel.loza@usc.es

<sup>3</sup> Dipartimento di Farmacia-Scienze del Farmaco, Università degli Studi di Bari Aldo Moro, Via E. Orabona 4, 70125 Bari, Italy; marco.catto@uniba.it

\* Correspondence: zoidis@pharm.uoa.gr; Tel.: +30-210-7274809

**Abstract:** Based on previously highlighted structural features, the development of highly selective 5-HT<sub>1A</sub> receptor inhibitors is closely linked to the incorporation of a 4-alkyl-1-arylpiperazine scaffold on them. In this paper, we present the synthesis of two new compounds bearing the 2-MeO-Ph-piperazine moiety linked via a three carbon atom linker to the amine group of 1-adamantanamine and memantine, respectively. Both were tested for their binding affinity against 5-HT<sub>1A</sub> receptor. *N*-(3-(4-(2-methoxyphenyl)piperazin-1-yl)propyl)tricyclo[3.3.1.1<sup>3,7</sup>]decan-1-amine fumarate (**8**) and *N*-(3-(4-(2-methoxyphenyl)piperazin-1-yl)propyl)-3,5-dimethyl-tricyclo[3.3.1.1<sup>3,7</sup>]decan-1-amine fumarate (**10**) proved to be highly selective ligands towards 5-HT<sub>1A</sub> receptor with a binding constant of 1.2 nM and 21.3 nM, respectively, while 5-carboxamidotriptamine (5-CT) (**2**) was used as an internal standard for this assay with a measured K<sub>i</sub> = 0.5 nM.

**Keywords:** serotonin receptors; 5-HT<sub>1A</sub> receptors; arylpiperazine inhibitors; carbocyclic rings; cage-like structures; blood-brain barrier; adamantane derivatives; NMR



**Citation:** Zoidis, G.; Loza, M.I.; Catto, M. Design, Synthesis and 5-HT<sub>1A</sub> Binding Affinity of *N*-(3-(4-(2-Methoxyphenyl)piperazin-1-yl)propyl)tricyclo[3.3.1.1<sup>3,7</sup>]decan-1-amine and *N*-(3-(4-(2-Methoxyphenyl)piperazin-1-yl)propyl)-3,5-dimethyl-tricyclo[3.3.1.1<sup>3,7</sup>]decan-1-amine. *Molbank* **2022**, *2022*, M1353. <https://doi.org/10.3390/M1353>

Academic Editor: Hideto Miyabe

Received: 22 February 2022

Accepted: 7 March 2022

Published: 10 March 2022

**Publisher's Note:** MDPI stays neutral with regard to jurisdictional claims in published maps and institutional affiliations.



**Copyright:** © 2022 by the authors. Licensee MDPI, Basel, Switzerland. This article is an open access article distributed under the terms and conditions of the Creative Commons Attribution (CC BY) license (<https://creativecommons.org/licenses/by/4.0/>).

## 1. Introduction

More than one-third of all drugs approved in 2017 by the US Food and Drug Administration (FDA) acted as G protein-coupled receptors (GPCRs) [1]. They are the most studied class of receptors due to their wide involvement in human diseases such as diabetes, obesity, Alzheimer's and several other central nervous system disorders [1,2]. Among the GPCRs belong also the serotonin class of receptors, specifically the serotonin 1A subtype (5-HT<sub>1A</sub>) [3]. This receptor has been tied to a variety of conditions (i.e., anxiety, mood, cognition) and its primary substrate is serotonin (Figure 1), a monoamine neurotransmitter that modulates brain function [3]. Recent therapeutic applications of receptor modulation have expanded towards prostate cancer, gastrointestinal and cardiopulmonary disorders and L-DOPA (Figure 1) induced dyskinesia [4]. 5-HT<sub>1A</sub> was one of the first discovered and still remains one of the most studied serotonin receptors. In the human brain they are abundant with localization both presynaptically on serotonergic neurons and postsynaptically in non-serotonergic neurons [5]. Dysfunctions associated with 5-HT<sub>1A</sub> neurotransmission have been directly implicated with stress response, aggressive behavior, psychiatric disorders, anxiety, depression and movement disorders [4,6].

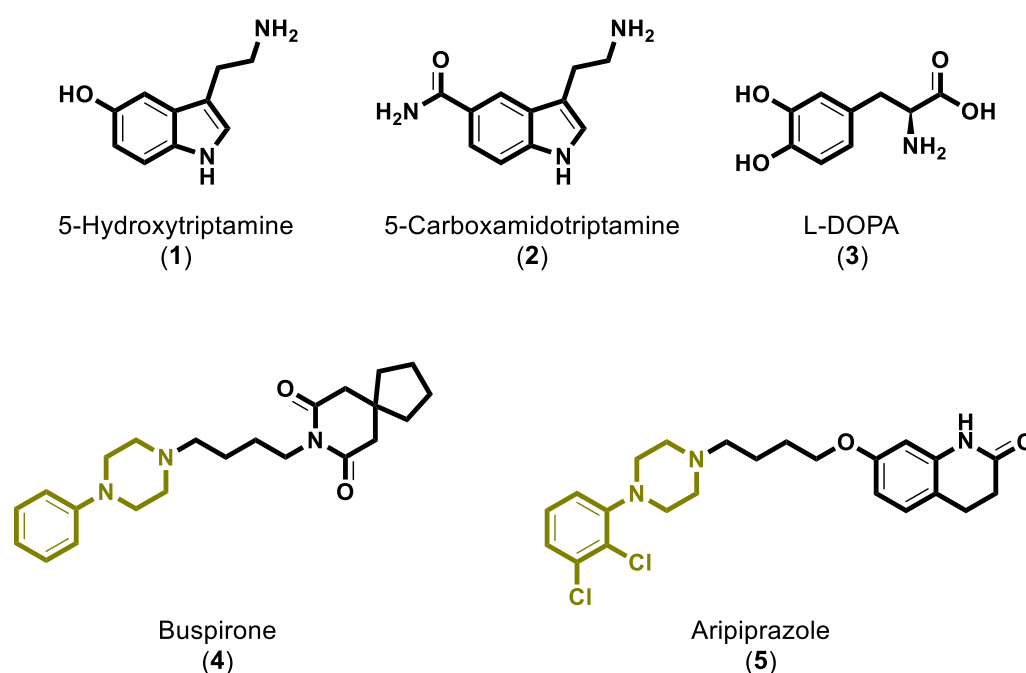


**Figure 1.** Chemical structures of serotonin and various arylpiperazine known inhibitors.

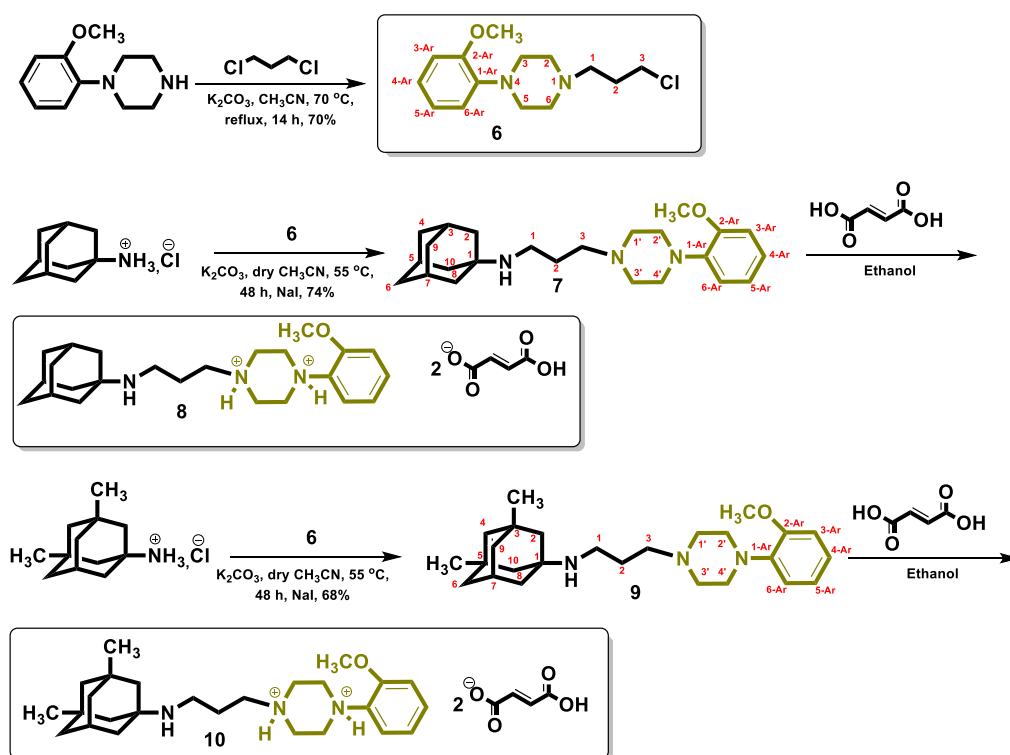
Despite all the progress with 5-HT<sub>1A</sub> receptors, very little was known about the inhibitor's binding mode in the absence of an available crystal structure, which was only recently published [7]. Therefore, drug design efforts were mostly based in structure-activity relationship data. Some of the most important identified class of drugs inhibiting the 5-HT<sub>1A</sub> receptor with increased selectivity contains an 4-alkyl-1-arylpiperazine moiety [8]. Representative structures (Figure 1) of marketed drugs are the anxiolytic buspirone [9] and the antipsychotic aripiprazole [10].

Herein we report the synthesis and biological evaluation of two new 5-HT<sub>1A</sub> inhibitors bearing the 2-MeO-Ph-piperazine moiety linked via a three carbon atom linker to cage-like structures of 1-adamantanamine and memantine. The introduction of this kind of bulky carbocyclic ring increases lipophilicity and biological membrane crossings [11]. Hence, the chemistry of adamantane continues to attract research interest due to the significant pharmacological activity of its derivatives [12–15].

## 2. Results and Discussion

### 2.1. Chemistry

The target compounds, (7) and (9), are obtained by following the synthetic procedure shown in Scheme 1. The key intermediate 1-(3-chloropropyl)-4-(2-methoxyphenyl)piperazine (6) was obtained by a nucleophilic substitution of 1,3-dichloropropane with 1-(2-methoxyphenyl)piperazine in dry acetonitrile under reflux. The latter (6) was condensed in dry acetonitrile in the presence of K<sub>2</sub>CO<sub>3</sub> and a catalytic amount of NaI either with amantadine hydrochloride to afford the target *N*-(3-(4-(2-methoxyphenyl)piperazin-1-yl)propyl)tricyclo[3.3.1.1<sup>3,7</sup>]decan-1-amine (7) or with memantine hydrochloride to yield the target *N*-(3-(4-(2-methoxyphenyl)piperazin-1-yl)propyl)-3,5-dimethyl-tricyclo[3.3.1.1<sup>3,7</sup>]decan-1-amine (9). Both analogues (7) and (9) were biologically tested as fumarate salts (8) and (10), respectively.



**Scheme 1.** Synthesis of the two lipophilic arylpiperazine derivatives (**8**) and (**10**).

## 2.2. Biological Activity

Target compounds were screened for their affinity against the serotonin 5-HT<sub>1A</sub> receptor. The exhibited activities were both in low nM magnitude, with (**8**) and (**10**) having a  $K_i$  of 1.2 nM and 21.3 nM respectively. Taken together, these data indicate that a (2-methoxyphenyl)piperazine motif delivers highly potent 5-HT<sub>1A</sub> ligands.

As an internal control for the 5-HT<sub>1A</sub> receptor, compound 5-CT (**2**) was used, based on Hamon et al. [16,17], which returned a  $K_i$  value of 0.5 nM.

Based on the recently revealed crystal structure of 5-HT<sub>1A</sub> receptor (Figure 2, PDB entry 7e2z [7]) with the presence of an arylpiperazine moiety bearing inhibitor (i.e., aripiprazole) such as our class of compounds, we were mobilized to perform a docking analysis in order to visualize important structural features. Therefore, we performed docking simulations for our compounds in the aripiprazole crystallized region. Residues defining the surface of study are Tyr96, Gln97, Phe112, Asp116, Val117, Cys120, Thr121, Ile189, Ser199, Phe361, Phe362, Ala365, Thr379, Ala383, Asn386, Trp387 and Tyr390. The software used for our experiments was the OpenEye Scientific Software, Inc., Santa Fe, NM, United States [18–20].

The new compound (**8**) presented in this study exhibits a 4-fold drop for its binding constant ( $K_i = 1.2$  nM) as measured over 5-HT<sub>1A</sub> receptor when compared to the value reported for the known drug aripiprazole ( $K_i = 5.0$  nM) [21]. The docking pose of (**8**) gave a  $-12.81$  Chemgauss4 scoring function. As shown in Figure 3, there are two major hydrogen bonds forming for the compound. One is between the protonated tertiary piperazine amine and Asp116, while the second is between the adamantane amine with Tyr390. On the other hand, (**10**) gave a  $-12.64$  Chemgauss4 scoring function with exactly the same interaction network (Figure 4), since the only difference in their structure is on the branched carbocycles. The measured constant in that case is approximately four-fold higher ( $K_i = 21.3$  nM). The difference in their affinities is due to the methyl groups of the memantine core, since one of the methyl groups is situated in the hydrophobic cavity formed by Ala93, Trp387 and Tyr390, while the other is directed towards Tyr96, introducing hindering effects. These results are in accordance with both in vitro and in silico results and they justify the high affinity of the 4-alkyl-1-arylpiperazine moiety towards 5-HT<sub>1A</sub> receptor [8].

Co-crystallized aripiprazole reveals only one important bond forming between the tertiary amine of the piperazine and Asp116 residue. Interestingly the etheric oxygen and the quinolinone do not show any apparent interactions with neighboring receptor residues, without excluding the possibility of a water-mediated bond network. However, as a fact there are no solvent molecules included in the deposited structure. Therefore it is rational that during the model validation, conducted by also performing the docking experiment for aripiprazole (scoring function  $-12.77$  Chemgauss4, see also supporting information Table S1), we witnessed a flipped quinolinone orientation (see Figure 5) in order for the molecule to form hydrogen bonds with Gln97 residue. This deviance from the co-crystallized pose resulted in an acceptable ( $\text{RMSD} \leq 2.0$ ) [22] but high RMSD value (i.e., 1.986) [23].

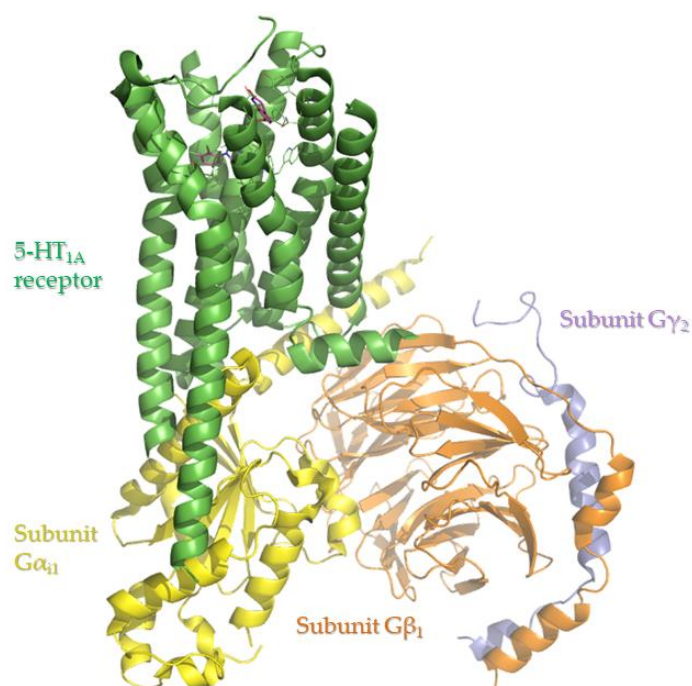


**Figure 2.** Crystal structure of the 7e2z PBD entry [7] of the 5-HT<sub>1A</sub> serotonin receptor in green colored cartoon representation and the respective complexed G-coupled proteins subunit G $\alpha_1$  in yellow, subunit G $\beta_1$  in orange and subunit G $\gamma_2$  in purple.

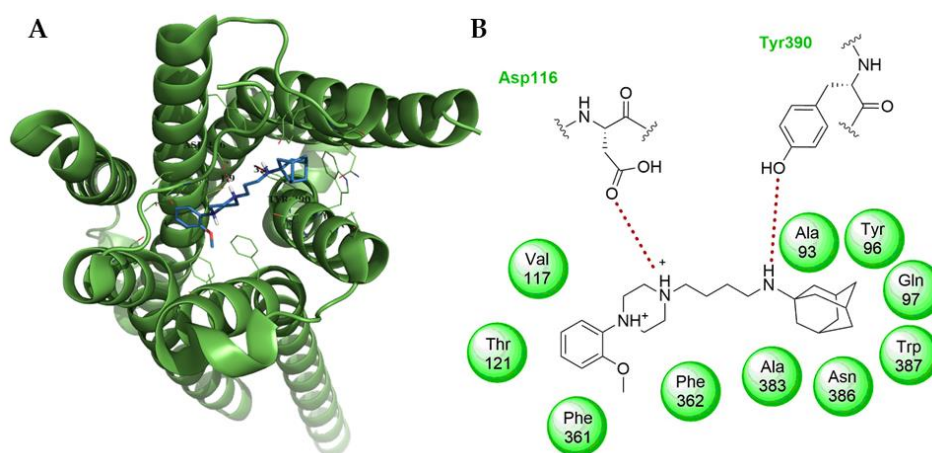


**Figure 3.** (A) Green cartoon representation of the 5-HT<sub>1A</sub> receptor with the presence of (8) at lowest scoring function binding mode as obtained from the software OpenEye in blue colored sticks, (B) 2D representation of (8) binding network forming as obtained from OpenEye software. Brick red dashed lines represent HB between receptor and (8).

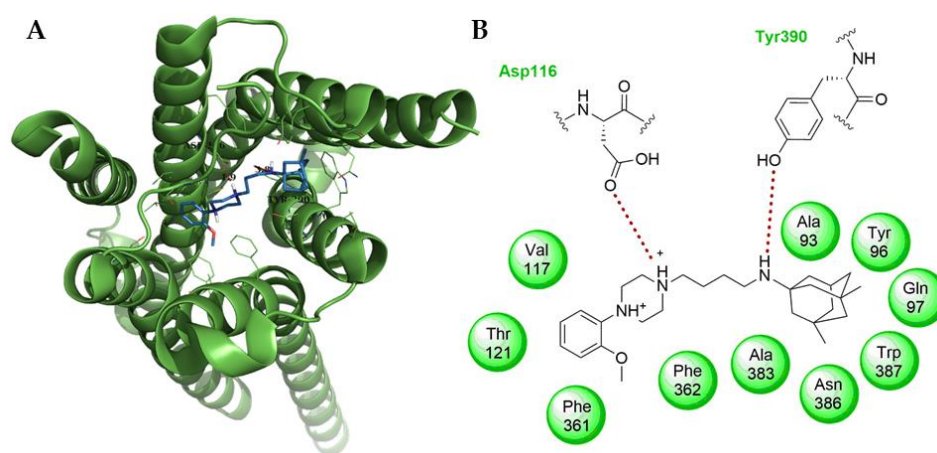


**Figure 4.** (A) Green cartoon representation of the 5-HT<sub>1A</sub> receptor with the presence of (10) at lowest scoring function binding mode as obtained from the software OpenEye in blue colored sticks, (B) 2D representation of (10) binding network forming as obtained from OpenEye software. Brick red dashed lines represent HB between receptor and (10).

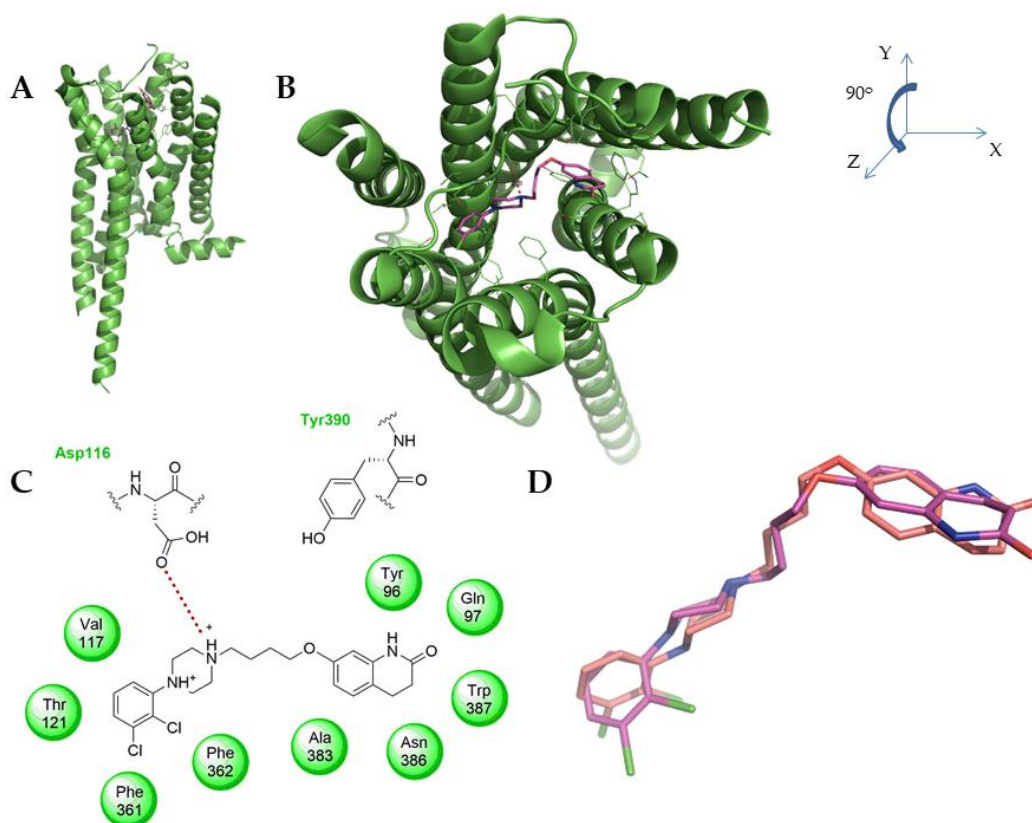


**Figure 5.** (A) Distant green representation of the 5-HT<sub>1A</sub> receptor with the presence of crystallized aripiprazole as magenta stick, (B) 90° rotation of the 5-HT<sub>1A</sub> receptor from the Y towards the Z axis revealing the whole interior of it, (C) 2D representation of aripiprazole crystal structure with the formed binding network, (D) overlay of co-crystallized aripiprazole as magenta colored sticks and docked solution of it as pink colored sticks.

To conclude, based on the scoring function order (see supporting information Table S1) and biological activity, these go hand in hand. Thus, the docking model showcases a desired mutual compatibility, providing important information for the mode of activity.

### 3. Materials and Methods

#### 3.1. Chemistry

Melting points were determined using a Büchi capillary apparatus and are uncorrected. NMR experiments (see Supplementary Materials) were performed to elucidate the structure and determine the purity of the newly synthesized compounds.  $^1\text{H-NMR}$  and 2D NMR spectra (COSY, HSQC-DEPT, HMBC) were recorded on a Bruker Ultrashiel™ Plus Avance III 600 spectrometer (150.9 MHz,  $^{13}\text{C-NMR}$ ) and a Bruker DRX400 spectrometer (100.62 MHz,  $^{13}\text{C-NMR}$ ). Chemical shifts  $\delta$  (delta) are reported in parts per million (ppm) downfield from the NMR solvent, with the tetramethylsilane or solvent (DMSO- $d_6$ ) as internal standard. Data processing, including Fourier transformation, baseline correction, phasing, peak peaking and integrations, were performed using MestReNova software v.12.0.0. Splitting patterns are designated as follows: s, singlet; d, doublet; t, triplet; dd, doublet of doublets; td, triplet of doublets; m, multiplet; complex m, complex multiplet. Coupling constants ( $J$ ) are expressed in units of Hertz (Hz). The spectra were recorded at 293 K (20 °C) unless otherwise specified. The solvent used to obtain the spectra was deuterated DMSO, DMSO- $d_6$  (quin, 2.50 ppm,  $^1\text{H-NMR}$ ; septet, 39.52 ppm,  $^{13}\text{C-NMR}$ ). Analytical thin-layer chromatography (TLC) was used to monitor the progress of the reactions, as well as to authenticate the compounds. TLCs were conducted on aluminum sheets precoated with normal-phase silica gel (Silica gel 60 F<sub>254</sub>, Merck, Darmstadt, Germany) (layer thickness 0.2 mm), aluminum sheets precoated with reverse phase silica gel (Silica gel 60 RP-18 F<sub>254</sub>S, Merck) and precoated aluminum oxide plates (TLC Aluminum oxide 60 F<sub>254</sub>, neutral). Developed plates were examined under a UV light source at wavelengths of 254 nm or after being stained by iodine vapors. The Retention factor ( $R_f$ ) of the newly synthesized compounds, which is equal to the distance migrated over the total distance covered by the solvent, was also measured on the chromatoplates. Elemental analyses (C, H, N) were performed by the Service Central de Microanalyse at CNRS (France) and were within  $\pm 0.4\%$  of the theoretical values. Elemental analysis results for the tested compounds correspond to  $>95\%$  purity. The HRMS spectra were acquired in the negative ionization mode, employing a QTOF-MS (Maxis Impact, Bruker Daltonics, Bremen, Germany) using a resolving power of 40,000. The commercial reagents were purchased from Alfa Aesar, Sigma-Aldrich and Merck, and were used without further purification. Solvent abbreviations: ACN, acetonitrile; AcOEt, ethyl acetate; Et<sub>2</sub>O, diethyl ether; EtOH, ethanol; MeOH, methanol.

#### 3.2. Synthesis

*1-(3-chloropropyl)-4-(2-methoxyphenyl)piperazine (6)*: A solution of 1, 3-dichloropropane (1.13 g, 10 mmol) in acetonitrile was added to a stirring solution of 1-(2-methoxyphenyl)-piperazine (1.28 g, 6.67 mmol) and K<sub>2</sub>CO<sub>3</sub> (2.69 g, 20.00 mmol) in 25 mL acetonitrile at 70 °C. The mixture was refluxed for 14 h. After it had been cooled to room temperature, the solvent was removed under vacuum. The crude product was purified by column chromatography on silica gel eluting with 1% MeOH in DCM ( $R_f = 0.75$ ). Light yellow oil, yield: 70%.

$^1\text{H-NMR}$  (400 MHz, CDCl<sub>3</sub>)  $\delta$  1.22 (t,  $J = 10.8$  Hz, 2H, 3-H), 1.84 (quintet,  $J = 10.8$  Hz, 2H, 2-H), 2.49 (t,  $J = 10.8$  Hz, 2H, 1-H), 2.69 (br s, 4H, 2,6 piperazine-H), 3.11 (br s, 4H, 3,5 piperazine-H), 3.83 (s, 3H, OCH<sub>3</sub>), 6.91–6.89 (m, 4H, 3,4,5,6 Ar-H) ppm.

$^{13}\text{C-NMR}$  (100 MHz, CDCl<sub>3</sub>)  $\delta$  23.7 (C<sub>2</sub>), 30.8 (C<sub>3</sub>), 50.3 (3,5 piperazine-C), 53.3 (2,6 piperazine-C), 55.2 (C<sub>1</sub>), 56.0 (OCH<sub>3</sub>), 111.0 (6-Ar-C), 120.9 (3-Ar-C), 122.9 (4,5-Ar-C), 141.0 (1-Ar-C), 152.1 (2-Ar-C) ppm.

*N-(3-(4-(2-methoxyphenyl)piperazin-1-yl)propyl)tricyclo[3.3.1.1<sup>3,7</sup>]decan-1-amine (7)*: Tricyclo[3.3.1.1<sup>3,7</sup>]decan-1-amine (Amantadine) hydrochloride (188.00 mg, 1.0 mmol) was stirred in dry acetonitrile (10 mL) with 3 equivalents of K<sub>2</sub>CO<sub>3</sub> (414.60 mg, 3.0 mmol) for 3 h at 55 °C. To this solution was added 1-(3-chloropropyl)-4-(2-methoxyphenyl)piperazine (6) (268.80 mg, 1.0 mmol) and a catalytic amount of NaI. The mixture was heated at reflux for 8 h. The precipitate was filtered and the filtrate was evaporated under vacuum to obtain a viscous oil residue, which was purified by column chromatography over silica gel eluting

first with ethyl acetate–methanol 9:1, 8:2, 7:3 and then ethyl acetate–methanol–triethylamine 70:29:1 to afford the title compound (7) as a colorless viscous oil (yield: 74%).

$^1\text{H-NMR}$  (600 MHz,  $\text{CDCl}_3$ )  $\delta$  1.55–1.70 (complex m, 14H, 2,4,6,8,9,10 Ad-H, 2-H), 2.05 (br s, 3H, 3,5,7 Ad-H), 2.46 (t,  $J = 7.2$  Hz, 2H, 3-H), 2.65 (br t,  $J = 4.8$  Hz, 6H, 2,6 piperazine-H, 1-H), 3.08 (br s, 4H, 3,5 piperazine-H), 3.85 (s, 3H,  $\text{OCH}_3$ ), 6.83–6.99 (m, 4H, 3,4,5,6 Ar-H) ppm.

$^{13}\text{C-NMR}$  (150 MHz,  $\text{CDCl}_3$ )  $\delta$  28.7 ( $\text{C}_2$ ), 30.5 ( $\text{C}_3, \text{C}_5, \text{C}_7$ -Ad), 37.6 ( $\text{C}_4, \text{C}_6, \text{C}_{10}$ -Ad), 40.1 ( $\text{C}_1$ ), 43.8 ( $\text{C}_2, \text{C}_8, \text{C}_9$ -Ad), 51.7 (3,5 piperazine-C), 53.7 ( $\text{C}_1$ -Ad), 54.6 ( $\text{C}_1$ ), 54.6 (2,6 piperazine-C), 55.2 ( $\text{C}_1$ ), 56.1 ( $\text{OCH}_3$ ), 58.1 ( $\text{C}_3$ ), 112.2 (6-Ar-C), 119.2 (3-Ar-C), 122.1 (4-Ar-C), 123.9 (5-Ar-C), 141.4 (1-Ar-C), 151.9 (2-Ar-C) ppm.

HRMS (ESI+)  $m/z$  calculated for  $\text{C}_{24}\text{H}_{37}\text{N}_3\text{O}$  is 383.2937 found ( $\text{M} + \text{H}$ ) $^+$  384.3018.

The fumarate salt (8) was prepared and obtained as a white crystalline solid and upon recrystallization from methanol–ether gave an mp: 219–221 °C (dec.). Anal. Calcd for  $\text{C}_{32}\text{H}_{45}\text{N}_3\text{O}_9$ : C, 62.42; H, 7.37; N, 6.82. Found: C, 62.70; H, 7.30; N, 7.01.

*N*-(3-(4-(2-methoxyphenyl)piperazin-1-yl)propyl)-3,5-dimethyl-tricyclo[3.3.1.1<sup>3,7</sup>]decan-1-amine (9): 3,5-Dimethyl-tricyclo[3.3.1.1<sup>3,7</sup>]decan-1-amine (Memantadine) hydrochloride (215.76 mg, 1.0 mmol) was stirred in dry acetonitrile (10 mL) with 3 equivalents of  $\text{K}_2\text{CO}_3$  (414.60 mg, 3.0 mmol) for 3 h at 55 °C. To this solution was added 1-(3-chloropropyl)-4-(2-methoxyphenyl)piperazine (6) (268.80 mg, 1.0 mmol) and a catalytic amount of NaI. The mixture was heated at reflux for 8 h. The precipitate was filtered and the filtrate was evaporated under vacuum to obtain a viscous oil residue, which was purified by column chromatography over silica gel eluting first with ethyl acetate–methanol 9:1, 8:2, 7:3 and then ethyl acetate–methanol–triethylamine 70:29:1 to afford the title compound (9) as a colorless viscous oil (yield: 68%).

$^1\text{H-NMR}$  (600 MHz,  $\text{CDCl}_3$ )  $\delta$  0.82 (s, 6H, 3- $\text{CH}_3$ , 5- $\text{CH}_3$ ), 1.09 (br s, 2H, 4 Ad-H), 1.22–1.38 (m, 8H, 2,6,9,10 Ad-H), 1.52 (br s, 2H, 8 Ad-H), 1.74 (br t,  $J = 9.6$  Hz, 2H, 2-H), 2.12 (s, 1H, 7 Ad-H), 2.48 (br t,  $J = 9.6$  Hz, 2H, 3-H), 2.67 (br s, 4H, 2,6 piperazine-H, 1-H), 2.72 (br t,  $J = 9.6$  Hz, 2H, 1-H), 3.07 (br s, 4H, 3,5 piperazine-H), 3.83 (s, 3H,  $\text{OCH}_3$ ), 6.82–6.99 (m, 4H, 3,4,5,6 Ar-H) ppm.

$^{13}\text{C-NMR}$  (150 MHz,  $\text{CDCl}_3$ )  $\delta$  26.2 ( $\text{C}_2$ ), 29.9 ( $\text{C}_7$ -Ad), 30.1 (3,5- $\text{CH}_3$ ), 32.2 ( $\text{C}_3, \text{C}_5$ -Ad), 39.8 ( $\text{C}_1$ ), 40.2 ( $\text{C}_8$ -Ad), 42.7 ( $\text{C}_6, \text{C}_{10}$ -Ad), 47.9 ( $\text{C}_2, \text{C}_9$ -Ad), 50.5 (3,5 piperazine-C), 50.7 ( $\text{C}_4$ -Ad), 53.3 (2,6 piperazine-C), 54.2 ( $\text{C}_1$ -Ad), 55.1 ( $\text{OCH}_3$ ), 57.4 ( $\text{C}_3$ ), 111.1 (6-Ar-C), 118.2 (3-Ar-C), 121.0 (4-Ar-C), 123.0 (5-Ar-C), 141.2 (1-Ar-C), 152.0 (2-Ar-C) ppm.

HRMS (ESI+)  $m/z$  calculated for  $\text{C}_{26}\text{H}_{40}\text{N}_3\text{O}$  is 410.3171 found ( $\text{M} + 2\text{H}$ ) $^+$  412.3303.

The fumarate salt (10) was prepared and obtained as a white crystalline solid and upon recrystallization from methanol–ether gave an mp: 208–210 °C (dec.). Anal. Calcd for  $\text{C}_{34}\text{H}_{49}\text{N}_3\text{O}_9$ : C, 63.43; H, 7.67; N, 6.53. Found: C, 63.62; H, 7.92; N, 6.42.

### 3.3. Computational

A library of the newly synthesized compounds (8) and (10) along with the known crystalized drug aripiprazole serving as control substance were compiled in both a smile formatted file (\*.smi) and a Sybyl MOL2 file (\*.mol2) using the free program Open Babel v3.1.1 [24]. Following this step, the smile library was subjected to conformer generation using Omega v4.1.0.0 software (OpenEye Scientific Software, Inc., Santa Fe, NM, USA; [www.eyesopen.com](http://www.eyesopen.com) (accessed on 10 March 2021) [25,26]. Experiments were then performed running on a basic laptop pc with an operating system of Windows 10 64-bit (Intel® Core™ i5-1035G1 1.00 GHz CPU processors, RAM 8 GB), using the OEDocking suite v4.0.0.0 programs (OpenEye Scientific Software, Inc., Santa Fe, NM, USA; [www.eyesopen.com](http://www.eyesopen.com) (accessed on 10 March 2021) [18–20]. Visualization of the results was performed over the software PyMol v1.4.1 [27].

### 3.4. Ligand and Protein Preparation

The 5-HT<sub>1A</sub> crystal structure (PDB entry 7e2z [7]) was downloaded over the protein databank [28]. The PDB file was prepared with the OEDocking suite program MAKE RECEPTOR v4.0.0.0 (OpenEye Scientific Software, Inc., Santa Fe, NM, USA; [www.eyesopen.com](http://www.eyesopen.com)).

com (accessed on 10 March 2021) [29,30] to provide the respective oedu extension file, which is used later in simulation experiments. The search space was centered around the crystalized small molecule inhibitor. This generated an initial box of 12,411 Å<sup>3</sup>, which after a balanced site-shape creation resulted in an inner docking space of 1026 Å<sup>3</sup> and an outer docking space of 1692 Å<sup>3</sup> for the protein. Neither residue modifications nor any constraints were implemented in the protein in the docking. The compiled SDF library contained all of the compounds (8), (10) and aripiprazole. Conformer generation took place with the use of Omega v4.1.0.0 software (OpenEye Scientific Software, Inc., Santa Fe, NM, USA; [www.eyesopen.com](http://www.eyesopen.com) (accessed on 10 March 2021)) [25,26] by setting a threshold of 600 structures with the flipping option turned on, and the docking was performed with the OEDocking suite program FRED v4.0.0.0 (OpenEye Scientific Software, Inc., Santa Fe, NM, USA; [www.eyesopen.com](http://www.eyesopen.com) (accessed on 10 March 2021)) [18,30]. Model calculations performed are produced by an Exhaustive Search Algorithm. Refinement of results was additionally performed in order to sort poses with standard options by OEDocking suite program Scorepose v4.0.0.0 (OpenEye Scientific Software, Inc., Santa Fe, NM, USA; [www.eyesopen.com](http://www.eyesopen.com) (accessed on 10 March 2021)) [18,19].

### 3.5. Model Confidence Experiment

The aripiprazole structure was included for confidence reasons regarding the model generated. Hence, the docked solution of the inhibitor was subjected to RMSD measurement online using the DockRMSD utility [23]. The input format of the corresponding structures are Sybyl MOL2.

### 3.6. Biology

Affinity of compounds was measured in cell membranes prepared in-house from a HEK-293 cell line transfected with human 5-HT<sub>1A</sub> receptors. 10 µg of membrane suspension were incubated with 2 nM [<sup>3</sup>H]-8-hydroxy-DPAT (PerkinElmer) in assay buffer (50 mM Tris-HCl, 5 mM MgSO<sub>4</sub>, 5 mM MgCl<sub>2</sub>; pH = 7.4) for 120 min at 37 °C in multiscreen FC 96-well plate (Millipore, Burlington, MA, USA). Non-specific binding was determined in the presence of 10 µM 5-HT. After the incubation time, samples were filtered and radioactivity was detected in a Microbeta Trilux reader.

Data were fitted to a 4-parameter logistic equation employing GraphPad Prism 5.1, and K<sub>i</sub> values were calculated by employing the Cheng-Prusoff equation [31].

## 4. Conclusions

*N*-(3-(4-(2-methoxyphenyl)piperazin-1-yl)propyl)tricyclo[3.3.1.1<sup>3,7</sup>]decan-1-amine (7) and *N*-(3-(4-(2-methoxyphenyl)piperazin-1-yl)propyl)-3,5-dimethyl-tricyclo[3.3.1.1<sup>3,7</sup>]decan-1-amine (9) were designed and synthesized as 5-HT<sub>1A</sub> ligands. The fumarate salts of both of them exhibited significant affinity for 5-HT<sub>1A</sub> (1.2 nM and 21.3 nM, respectively), and thus these compounds could be useful for researching the physiological and pharmacological roles of this receptor. The docking analysis visualized some important structural features and interactions, providing useful information for the mode of activity that will help the future design of this class of compounds. Structures of the targeted compounds were determined using <sup>1</sup>H-NMR, <sup>13</sup>C-NMR, HSQC, HMBC, COSY, elemental analysis and HRMS.

**Supplementary Materials:** The following are available online. Copies of NMR spectra; Figure S1: (A) Distant green representation of the 5-HT<sub>1A</sub> receptor with the presence of crystallized Aripiprazole as magenta stick, (B) 90° rotation of the 5-HT<sub>1A</sub> receptor from the Y towards the Z axis revealing the whole interior of it, (C) 2D representation of Aripiprazole crystal structure with the formed binding network, (D) overlay of co-crystalized Aripiprazole as magenta colored sticks and docked solution of it as pink colored sticks. Brick red dashed lines represent HB between protein and the substrate, Table S1: Molecular modeling results. Comparative presentation of in vitro & in silico results of compounds versus 5-HT<sub>1A</sub> receptor.

**Author Contributions:** Conceptualization, methodology, formal analysis, investigation, resources, data curation, writing—original draft preparation, writing—review and editing, supervision, project administration, funding acquisition, G.Z.; conceptualization and draft editing, M.C.; investigation, data curation and draft editing M.I.L. All authors have read and agreed to the published version of the manuscript.

**Funding:** This research was funded by Empirikion Foundation.

**Institutional Review Board Statement:** Not applicable.

**Informed Consent Statement:** Not applicable.

**Data Availability Statement:** Not applicable.

**Acknowledgments:** The authors would like to thank Openeye Scientific Software, Inc., Santa Fe, NM, USA; [www.eyesopen.com](http://www.eyesopen.com) (accessed on 10 March 2021), for providing an academic license of their programs.

**Conflicts of Interest:** The authors declare no conflict of interest.

## References

1. Hauser, A.S.; Attwood, M.M.; Rask-Andersen, M.; Schioth, H.B.; Gloriam, D.E. Trends in GPCR drug discovery: New agents, targets and indications. *Nat. Rev. Drug Discov.* **2017**, *16*, 829–842. [[CrossRef](#)]
2. Huang, Y.; Todd, N.; Thathiah, A. The role of GPCRs in neurodegenerative diseases: Avenues for therapeutic intervention. *Curr. Opin. Pharmacol.* **2017**, *32*, 96–110. [[CrossRef](#)]
3. Polter, A.M.; Li, X. 5-HT<sub>1A</sub> receptor-regulated signal transduction pathways in brain. *Cell. Signal.* **2010**, *22*, 1406–1412. [[CrossRef](#)]
4. Staron, J.; Bugno, R.; Hogendorf, A.S.; Bojarski, A.J. 5-HT<sub>1A</sub> receptor ligands and their therapeutic applications: Review of new patents. *Expert Opin. Ther. Pat.* **2018**, *28*, 679–689. [[CrossRef](#)]
5. Albert, P.R.; Vahid-Ansari, F. The 5-HT<sub>1A</sub> receptor: Signaling to behavior. *Biochimie* **2019**, *161*, 34–45. [[CrossRef](#)]
6. Popova, N.K.; Naumenko, V.S. 5-HT<sub>1A</sub> receptor as a key player in the brain 5-HT system. *Rev. Neurosci.* **2013**, *24*, 191–204. [[CrossRef](#)]
7. Xu, P.; Huang, S.; Zhang, H.; Mao, C.; Zhou, X.E.; Cheng, X.; Simon, I.A.; Shen, D.D.; Yen, H.Y.; Robinson, C.V.; et al. Structural insights into the lipid and ligand regulation of serotonin receptors. *Nature* **2021**, *592*, 469–473. [[CrossRef](#)]
8. Perrone, R.; Berardi, F.; Colabufo, N.A.; Leopoldo, M.; Tortorella, V.; Fiorentini, F.; Olgiati, V.; Ghiglieri, A.; Govoni, S. High affinity and selectivity on 5-HT<sub>1A</sub> receptor of 1-aryl-4-[1-tetralin]alkylpiperazines. 2. *J. Med. Chem.* **1995**, *38*, 942–949. [[CrossRef](#)]
9. Napoliello, M.J.; Domantay, A.G. Buspirone: A Worldwide Update. *Br. J. Psychiatry* **2018**, *159*, 40–44. [[CrossRef](#)]
10. Di Sciascio, G.; Riva, M.A. Aripiprazole: From pharmacological profile to clinical use. *Neuropsychiatr. Dis. Treat.* **2015**, *11*, 2635–2647. [[CrossRef](#)]
11. Giannakopoulou, E.; Pardali, V.; Skrettas, I.; Zoidis, G. Transesterification instead of N-Alkylation: An Intriguing Reaction. *ChemistrySelect* **2019**, *4*, 3195–3198. [[CrossRef](#)]
12. Kolocouris, N.; Zoidis, G.; Fytas, C. Facile synthetic routes to 2-oxo-1-adamantanalkanoic acids. *Synlett* **2007**, *2007*, 1063–1066. [[CrossRef](#)]
13. Zoidis, G.; Benaki, D.; Myriantopoulos, V.; Naesens, L.; De Clercq, E.; Mikros, E.; Kolocouris, N. Synthesis of 1, 2-annulated adamantane heterocycles: Structural determination studies of a bioactive cyclic sulfite. *Tetrahedron Lett.* **2009**, *50*, 2671–2675. [[CrossRef](#)]
14. Tsatsaroni, A.; Zoidis, G.; Zoumpoulakis, P.; Tsoinina, A.; Taylor, M.C.; Kelly, J.M.; Fytas, G. An E/Z conformational behaviour study on the trypanocidal action of lipophilic spiro carbocyclic 2,6-diketopiperazine-1-acetohydroxamic acids. *Tetrahedron Lett.* **2013**, *54*, 3238–3240. [[CrossRef](#)]
15. Fytas, C.; Zoidis, G.; Fytas, G. A facile and effective synthesis of lipophilic 2, 6-diketopiperazine analogues. *Tetrahedron* **2008**, *64*, 6749–6754. [[CrossRef](#)]
16. Hamon, M. The main features of central 5-HT<sub>1A</sub> receptors. In *Serotonergic Neurons and 5-HT Receptors in the CNS*; Springer: Berlin/Heidelberg, Germany, 2000; pp. 239–268.
17. Hamon, M.; Lanfumey, L.; El Mestikawy, S.; Boni, C.; Miquel, M.-C.; Bolanos, F.; Schechter, L.; Gozlan, H. The main features of central 5-HT<sub>1</sub> receptors. *Neuropsychopharmacol. Off. Publ. Am. Coll. Neuropsychopharmacol.* **1990**, *3*, 349–360.
18. McGann, M. FRED pose prediction and virtual screening accuracy. *J. Chem. Inf. Model.* **2011**, *51*, 578–596. [[CrossRef](#)]
19. McGaughey, G.B.; Sheridan, R.P.; Bayly, C.I.; Culberson, J.C.; Kreatsoulas, C.; Lindsley, S.; Maiorov, V.; Truchon, J.F.; Cornell, W.D. Comparison of topological, shape, and docking methods in virtual screening. *J. Chem. Inf. Modeling* **2007**, *47*, 1504–1519. [[CrossRef](#)]
20. McGann, M.R.; Almond, H.R.; Nicholls, A.; Grant, J.A.; Brown, F.K. Gaussian docking functions. *Biopolymers* **2003**, *68*, 76–90. [[CrossRef](#)]
21. Shapiro, D.A.; Renock, S.; Arrington, E.; Chiodo, L.A.; Liu, L.X.; Sibley, D.R.; Roth, B.L.; Mailman, R. Aripiprazole, a novel atypical antipsychotic drug with a unique and robust pharmacology. *Neuropsychopharmacology* **2003**, *28*, 1400–1411. [[CrossRef](#)]
22. Ramírez, D.; Caballero, J. Is It Reliable to Take the Molecular Docking Top Scoring Position as the Best Solution without Considering Available Structural Data? *Molecules* **2018**, *23*, 1038. [[CrossRef](#)]

23. Bell, E.W.; Zhang, Y. DockRMSD: An open-source tool for atom mapping and RMSD calculation of symmetric molecules through graph isomorphism. *J. Cheminform.* **2019**, *11*, 40. [[CrossRef](#)]
24. O'Boyle, N.M.; Banck, M.; James, C.A.; Morley, C.; Vandermeersch, T.; Hutchison, G.R. Open Babel: An open chemical toolbox. *J. Cheminform.* **2011**, *3*, 33. [[CrossRef](#)]
25. Hawkins, P.C.; Nicholls, A. Conformer generation with OMEGA: Learning from the data set and the analysis of failures. *J. Chem. Inf. Model.* **2012**, *52*, 2919–2936. [[CrossRef](#)]
26. Hawkins, P.C.; Skillman, A.G.; Warren, G.L.; Ellingson, B.A.; Stahl, M.T. Conformer generation with OMEGA: Algorithm and validation using high quality structures from the Protein Databank and Cambridge Structural Database. *J. Chem. Inf. Model.* **2010**, *50*, 572–584. [[CrossRef](#)]
27. *The PyMOL Molecular Graphics System*; Version 1.4.1; Schrodinger, LLC: New York, NY, USA.
28. Berman, H.M.; Westbrook, J.; Feng, Z.; Gilliland, G.; Bhat, T.N.; Weissig, H.; Shindyalov, I.N.; Bourne, P.E. The Protein Data Bank. *Nucleic Acids Res.* **2000**, *28*, 235–242. [[CrossRef](#)]
29. Kelley, B.P.; Brown, S.P.; Warren, G.L.; Muchmore, S.W. POSIT: Flexible Shape-Guided Docking for Pose Prediction. *J. Chem. Inf. Model.* **2015**, *55*, 1771–1780. [[CrossRef](#)]
30. McGann, M. FRED and HYBRID docking performance on standardized datasets. *J. Comput.-Aided Mol. Des.* **2012**, *26*, 897–906. [[CrossRef](#)]
31. Cheng, Y.C.; Prusoff, W.H. Relationship between the inhibition constant ( $K_i$ ) and the concentration of inhibitor which causes 50 percent inhibition ( $IC_{50}$ ) of an enzyme reaction. *Biochem. Pharmacol.* **1973**, *22*, 3099–3108. [[CrossRef](#)]